Genetic structure of prey populations underlies the geographic mosaic of arms race coevolution

Authors: Michael T.J. Hague[1*], Amber N. Stokes[2], Chris R. Feldman[3], Edmund D. Brodie, Jr.[4], Edmund D. Brodie III[5]

Affiliations:

[1] Department of Biological Sciences, University of Montana, Missoula, MT.

[2] Department of Biology, California State University, Bakersfield, CA.

[3] Department of Biology, University of Nevada, Reno, NV.

[4] Department of Biology, Utah State University, Logan, UT.

[5] Department of Biology, University of Virginia, Charlottesville, VA.

[*] Correspondence to:

Michael T.J. Hague

Department of Biological Sciences, University of Montana

32 Campus Dr. HS 104, Missoula, MT 59812

Tel: (406) 243-2182

Email: michael.hague@mso.umt.edu

Short title: Prey structure mosaic of coevolution

Abstract:

Reciprocal adaptation is the hallmark of arms race coevolution, but the symmetry of evolutionary change in each species is often untested even in the best-studied battles between natural enemies. We tested whether prey and predator exhibit a symmetrical pattern of local co-adaptation in the classic example of a geographic mosaic of coevolution between toxic newts (*Taricha granulosa*) and resistant garter snakes (*Thamnophis sirtalis*). Contrary to conventional wisdom, landscape variation in the newt toxin TTX is best predicted by neutral population divergence and not predator resistance, whereas snake resistance is clearly explained by prey toxin levels. Prey populations structure variation in levels of TTX, which in turn structures selection on predators—implying that neutral processes including gene flow, rather than reciprocal adaptation, are the primary source of variation across the coevolutionary mosaic.

Main Text:

Coevolutionary dynamics result from the reciprocal selection generated between interacting species (*1*, *2*). Adaptation and counter-adaptation occur at the phenotypic interface of coevolution, the traits in each species that mediate interactions (*3*, *4*). Because species interactions and their fitness consequences vary spatially, heterogeneity in the form of reciprocal selection is expected to generate a geographic mosaic of coevolution in which phenotypes of both species covary due to local conditions (*2*, *5*–*7*). Coevolving species often exhibit matched trait variation across the landscape, for example, in seed traits and their predators (*5*, *7*) or host and pathogen genotypes (*8*, *9*), a pattern typically interpreted as a signature of local co-adaptation.

However, a geographic mosaic of matched phenotypes may not be solely the result of reciprocal co-adaptation (*10, 11*). A simpler, non-adaptive explanation for matched trait variation involves the spatial population structure and ancestry of each species. Common barriers to dispersal or a shared biogeographic history, for example, could structure phenotypic divergence congruently in co-occurring species (*12*). Only when phenotypic variation deviates from the neutral expectations of population structure in both species can we infer local adaptation in the geographic mosaic of coevolution (*10*). Otherwise, drift, gene flow, and phylogeography provide a parsimonious explanation for patterns of divergence across the landscape.

We tested whether neutral processes account for localized trait matching in a textbook example of a geographic mosaic of coevolution, the arms race between deadly newt prey and their resistant snake predators. In western North America, rough-skinned newts (*Taricha granulosa*) secrete the deadly neurotoxin tetrodotoxin (TTX), which binds to the outer pore of voltage-gated sodium channels (Na_V) and prevents the initiation of action potentials (*13*, *14*).

Common garter snakes (*Thamnophis sirtalis*) exhibit resistance to TTX that is largely due to specific amino acid substitutions in the fourth domain pore-loop (DIV p-loop) of the skeletal muscle sodium channel ($Na_V1.4$) that disrupt toxin-binding (Fig. 1) (*15*, *16*). Channel-level TTX resistance conferred by each allele in the DIV p-loop is tightly correlated with muscle and whole-animal levels of phenotypic resistance in *Th. sirtalis* (*15–17*). TTX-resistant alleles occur at high frequency in coevolutionary "hotspots" with highly toxic newts, but are largely absent in surrounding "coldspots" where newts are non-toxic, creating a putative mosaic of local adaptation in which predator and prey have roughly matched abilities at the interface of toxin-binding (*11*, *18*, *19*).

We conducted fine-scale population sampling of newts (n=138) and garter snakes (n=169) along a latitudinal transect of nine locations on the Pacific Coast in Washington and Oregon (USA) that spans the geographic mosaic (Fig. 1, Table S1), ranging from low levels of newt toxin and snake resistance (northern Washington) to a hotspot of extreme escalation in both species (central Oregon). At each location, we characterized levels of TTX in newt populations and TTX resistance in garter snakes, including whole-animal phenotypic resistance and $Na_V1.4$ channel genotypes. We then compared these data to neutral patterns of population genomic variation using single nucleotide polymorphisms (SNPs) in each species.

Spatial patterns of newt TTX and snake resistance were broadly consistent with previous work suggesting arms race coevolution has led to closely matched phenotypes in each species (*11*). TTX levels ($\mu g/cm^2$) of newts varied by population (ANOVA; $F[8,114]=37.43$, $p<0.001$) and by sex ($F[1,114]=4.37$, $p=0.039$) along the latitudinal transect (Fig. 1; Table S1). TTX resistance (50% MAMU dose) of snakes also varied by population (according to non-overlapping 95% confidence intervals; Fig. 1; Table S1) and was closely correlated with prey

toxins (Table 1). The presence of TTX-resistant alleles in the $Na_V1.4$ channel co-varied with phenotypic resistance in garter snakes, such that pairwise F_{ST} divergence at the DIV p-loop was correlated with population divergence in phenotypic resistance (Mantel test, r=0.47, p=0.032).

Variation in levels of newt TTX, however, was best predicted by neutral population divergence, calling into question whether the covariance between prey toxins and predator resistance is a result of co-adaptation to local conditions in the geographic mosaic. We used neutral SNPs to assess population genetic structure in prey and predator and found a pattern of isolation-by-distance (IBD) in both species (distance-based redundancy analysis; newts, F=-38.528, p=0.002; snakes, F=22.021, p=0.001). Principal coordinate (PCoA) and Bayesian clustering (STRUCTURE) analyses indicated that newts and snakes each have a distinct spatial pattern of population structure along the transect (Fig. 2). We generated distance matrices to test whether phenotypic divergence in one species (e.g., newt TTX levels) is best explained by (1) neutral genomic divergence (pairwise F_{ST}; Table S3) or (2) phenotypic divergence in the natural enemy (snake resistance). In univariate regressions, population divergence in the TTX level of newts was strongly predicted by neutral F_{ST} divergence (R^2=0.414), as well as TTX resistance of garter snakes (R^2=0.274; Table 1). F_{ST} divergence remained significant in the multiple regression, indicating that population structure of newts predicts TTX levels, even after controlling for TTX resistance of the predator (which was only marginally significant; p=0.065). In contrast, garter snake resistance was strictly predicted by newt toxins and not neutral F_{ST} divergence. Both phenotypic resistance and F_{ST} divergence at the DIV p-loop (the site of toxin-binding in $Na_V1.4$) were uncorrelated with neutral F_{ST} values in garter snakes (Table 1). These results imply that neutral genetic divergence structures population variation in levels of the prey toxin, which in turn predicts TTX resistance in predator populations. The geographic structure of

103 newt populations appears to be so influential to spatial dynamics that divergence in garter snake
104 phenotypic resistance and F_{ST} at the DIV p-loop are both significantly predicted by neutral F_{ST}
105 divergence of newts (Table 1).

106 Clinal variation in the TTX level of newts is highly congruent with neutral genomic
107 variation based on the PCoA (Fig. 3) and Bayesian clustering analyses (Fig. S2). TTX resistance
108 of garter snakes, in contrast, clearly deviates from neutral expectations to track variation in prey
109 toxins. Cline-fitting analyses show that prey toxin levels and predator resistance are tightly
110 matched along the 611 km transect; the geographic center points of each cline are located just 64
111 km apart and do not differ statistically. The cline center of TTX-resistant alleles in snakes is also
112 located nearby, although it differed statistically from the center of newt TTX. Despite similar
113 phenotypic clines in prey and predator, variation in levels of newt toxin showed an even tighter
114 match to clinal variation in neutral population structure. The center points of the TTX and neutral
115 clines were located only 19 km apart. PC 1 from the PCoA was a strong predictor of variation in
116 TTX levels (linear model; t-value=5.682, $p<0.001$), even after controlling for the effect of TTX
117 resistance of garter snakes (Supplemental Materials, Table S5). Conversely, variation in
118 phenotypic resistance and TTX-resistant alleles in snakes both deviated significantly from the
119 neutral cline (Fig. 3), such that resistance was not predicted by PCs 1 or 2 from the PCoA (Table
120 S5). The center points of the snake phenotypic resistance and neutral clines were located a
121 distant 310 km apart.

122 Levels of prey toxin and predator resistance are tightly matched across the landscape, but
123 this pattern does not appear to be the primary result of local co-adaptation in the arms race.
124 Although predator resistance is geographically structured by a signature of local adaptation to
125 prey, levels of prey toxin are clearly structured according to neutral population divergence.

126 These results imply that mosaic variation in newt toxins is largely explained by non-adaptive
127 processes, such as drift and historical biogeography, rather than spatially variable adaptation. For
128 example, latitudinal patterns of newt TTX and neutral divergence are both consistent with a
129 population history of northward expansion after the Pleistocene glacial period (*20*). Toxin levels
130 in the newts may have been under strong selection in the past, particularly at the southern end of
131 the transect, but now it is predominantly subject to neutral processes like drift and gene flow.
132 The asymmetric signatures of adaptation we observed in prey and predator may reflect
133 differences in the mechanisms that underlie phenotypic variation in each species. The
134 evolutionary response in newts may be obscured by environmental effects that disproportionally
135 contribute to variance in TTX levels compared to resistance of snakes. Little is known about the
136 production of TTX, but some researchers suggest exogenous factors, like environmentally-
137 derived precursors, may affect the ability of newts to synthesize or sequester TTX (*21*, *22*).
138 Evidence from the California newt (*Ta. torosa*) suggests TTX levels could also be a plastic
139 response to sustained stressful conditions such as predation (*23*). On the other hand, TTX
140 resistance in garter snakes is largely due to a small number of amino acid changes to the p-loops
141 of the $Na_V1.4$ channel (*15*–*17*, *19*). These large-effect mutations could make TTX resistance
142 more evolutionarily labile than toxicity, permitting rapid local adaptation in predator populations
143 (*11*, *17*).
144 Asymmetric patterns of evolution could also arise from a selective imbalance associated
145 with the interactions between prey and predator. In antagonistic interactions, the species under
146 more intense selection is generally expected to be better adapted to local conditions (*24*). While
147 prey are typically thought to experience stronger selection than their predators (the “life-dinner
148 principle”) (*25*), this asymmetry may be reversed when prey contain deadly toxins like TTX (*3*).

149 In fact, populations in central Oregon are the most toxic newts known (*11*), so non-resistant
150 predators should experience severe fitness consequences.

151 Non-adaptive processes of drift and gene flow provide a parsimonious explanation for
152 landscape-level patterns of variation in newt TTX, but the extreme exaggeration in levels of prey
153 toxins and predator resistance in some locations is likely the result of arms race coevolution.
154 Reciprocal coevolution may be ongoing in hotspots, like central Oregon, while levels of newt
155 TTX in surrounding regions are spatially structured according to patterns of gene flow. This
156 overall pattern establishes the important role of "trait remixing", a largely untested component of
157 the geographic mosaic theory that is thought to generate spatial variation in species interactions
158 (*2*, *10*). The neutral processes of drift and gene flow (termed "trait remixing") are predicted to
159 continually alter the spatial distribution of allelic and phenotypic variation, potentially interfering
160 with local selection. Gene flow outwards from hotspots of coevolution is predicted to alter
161 dynamics in surrounding populations (*26*, *27*), and if gene flow is high, the population with the
162 strongest reciprocal effects on fitness is expected to dictate broader landscape patterns of trait
163 variation (*24*, *26*, *28*). The homogenizing effects of gene flow may be less influential in snake
164 populations due to the simple genetic basis of TTX resistance or strong selection on predators.

165 Our results underscore that landscape patterns of phenotypic matching in natural enemies
166 are not the inherent result of coevolution (*10*). External factors such as abiotic conditions (*29*),
167 evolutionary constraints (*30*), or interactions with other species (*31*) are likely to have unique
168 effects on the evolution of prey and predator. In the newt-snake arms race, it appears that neutral
169 processes and population structure disproportionally affect toxin levels in newts, which in turn,
170 determines mosaic patterns of phenotypic variation in both species across the landscape. The
171 evolutionary response to selection at the phenotypic interface is almost certain to differ in two

172 interacting species—so much so that coevolution may not always be the most parsimonious
173 explanation for observed patterns of phenotypic divergence and trait matching across the
174 geographic mosaic.
175

176 **References and Notes:**

177 1. D. H. Janzen, When is it coevolution? *Evolution* (1980).

178 2. J. N. Thompson, *The Geographic Mosaic of Coevolution* (University of Chicago Press,
179 Chicago, 2005).

180 3. E. D. Brodie III, E. D. Brodie Jr, Predator-prey arms races. *BioScience*. **49**, 557–568
181 (1999).

182 4. E. D. Brodie III, B. J. Ridenhour, Reciprocal selection at the phenotypic interface of
183 coevolution. *Integr. Comp. Biol*. **43**, 408–418 (2003).

184 5. C. W. Benkman, T. L. Parchman, A. Favis, A. M. Siepielski, Reciprocal selection causes a
185 coevolutionary arms race between crossbills and lodgepole pine. *Am. Nat.* **162**, 182–194
186 (2003).

187 6. A. R. Zangerl, M. R. Berenbaum, Phenotype matching in wild parsnip and parsnip
188 webworms: causes and consequences. *Evolution*. **57**, 806–815 (2003).

189 7. H. Toju, S. Ueno, F. Taniguchi, T. Sota, Metapopulation structure of a seed-predator weevil
190 and its host plant in arms race coevolution. *Evolution*. **65**, 1707–1722 (2011).

191 8. C. M. Lively, M. F. Dybdahl, Parasite adaptation to locally common host genotypes.
192 *Nature*. **405**, 679 (2000).

193 9. P. H. Thrall, J. Burdon, J. D. Bever, Local adaptation in the *Linum marginale—Melampsora*
194 *lini* host-pathogen interaction. *Evolution*. **56**, 1340–1351 (2002).

195 10. R. Gomulkiewicz *et al.*, Dos and don'ts of testing the geographic mosaic theory of
196 coevolution. *Heredity*. **98**, 249–258 (2007).

197 11. C. T. Hanifin, E. D. Brodie, Jr., E. D. Brodie III, Phenotypic mismatches reveal escape
198 from arms-race coevolution. *PLoS Biol*. **6**, e60 (2008).

199 12. N. G. Swenson, D. J. Howard, A. E. M. E. Hellberg, E. J. B. Losos, Clustering of contact
200 zones, hybrid zones, and phylogeographic breaks in North America. *Am. Nat.* **166**, 581–591
201 (2005).

202 13. H. A. Fozzard, G. M. Lipkind, The tetrodotoxin binding site is within the outer vestibule of
203 the sodium channel. *Mar. Drugs*. **8**, 219–234 (2010).

204 14. D. B. Tikhonov, B. S. Zhorov, Architecture and pore block of Eukaryotic voltage-gated
205 sodium channels in view of NavAb bacterial sodium channel structure. *Mol. Pharmacol.*
206 **82**, 97–104 (2012).

207 15. S. Geffeney, E. D. Brodie, Jr., P. C. Ruben, E. D. Brodie III, Mechanisms of adaptation in a
208 predator-prey arms race: TTX-resistant sodium channels. *Science*. **297**, 1336–1339 (2002).

16. S. L. Geffeney, E. Fujimoto, E. D. Brodie III, E. D. Brodie, Jr., P. C. Ruben, Evolutionary diversification of TTX-resistant sodium channels in a predator-prey interaction. *Nature*. **434**, 759–763 (2005).

17. C. R. Feldman, E. D. Brodie, Jr., E. D. Brodie III, M. E. Pfrender, Genetic architecture of a feeding adaptation: garter snake (*Thamnophis*) resistance to tetrodotoxin bearing prey. *Proc. R. Soc. B Biol. Sci.* **277**, 3317–3325 (2010).

18. E. D. Brodie, Jr., B. J. Ridenhour, E. D. Brodie III, The evolutionary response of predators to dangerous prey: hotspots and coldspots in the geographic mosaic of coevolution between garter snakes and newts. *Evolution*. **56**, 2067–2082 (2002).

19. M. T. J. Hague, C. R. Feldman, E. D. Brodie, Jr., E. D. Brodie III, Convergent adaptation to dangerous prey proceeds through the same first-step mutation in the garter snake *Thamnophis sirtalis*. *Evolution*. **71**, 1504–1518 (2017).

20. B. J. Ridenhour, E. D. Brodie, Jr., E. D. Brodie III, Patterns of genetic differentiation in *Thamnophis* and *Taricha* from the Pacific Northwest. *J. Biogeogr*. **34**, 724–735 (2007).

21. M. Yotsu, M. Iorizzi, T. Yasumoto, Distribution of tetrodotoxin, 6-epitetrodotoxin, and 11-deoxytetrodotoxin in newts. *Toxicon*. **28**, 238–241 (1990).

22. T. Yasumoto, M. Yotsu-Yamashita, Chemical and etiological studies on tetrodotoxin and its analogs. *Toxin Rev.* **15**, 81–90 (1996).

23. G. M. Bucciarelli, H. B. Shaffer, D. B. Green, L. B. Kats, An amphibian chemical defense phenotype is inducible across life history stages. *Sci. Rep.* **7** (2017).

24. S. Gandon, Local adaptation and the geometry of host–parasite coevolution. *Ecol. Lett.* **5**, 246–256 (2002).

25. R. Dawkins, J. R. Krebs, Arms races between and within species. *Proc. R. Soc. Lond. B Biol. Sci.* **205**, 489–511 (1979).

26. R. Gomulkiewicz, J. N. Thompson, R. D. Holt, Nuismer Scott L., M. E. Hochberg, Hot spots, cold spots, and the geographic mosaic theory of coevolution. *Am. Nat.* **156**, 156–174 (2000).

27. J. N. Thompson, S. L. Nuismer, R. Gomulkiewicz, Coevolution and maladaptation. *Integr. Comp. Biol.* **42**, 381–387 (2002).

28. S. Gandon, Y. Michalakis, Local adaptation, evolutionary potential and host–parasite coevolution: interactions between migration, mutation, population size and generation time. *J. Evol. Biol.* **15**, 451–462 (2002).

29. S. G. Johnson, C. D. Hulsey, F. J. G. León, Spatial mosaic evolution of snail defensive traits. *BMC Evol. Biol.* **7**, 1–11 (2007).

30. M. T. J. Hague *et al.*, Large-effect mutations generate trade-off between predatory and locomotor ability during arms race coevolution with deadly prey. *Evol. Lett.* **2**, 406–416 (2018).

31. C. W. Benkman, W. C. Holimon, J. W. Smith, The influence of a competitor on the geographic mosaic of coevolution between crossbills and lodgepole pine. *Evolution*. **55**, 282–294 (2001).

32. B. G. Gall *et al.*, Tetrodotoxin levels in larval and metamorphosed newts (*Taricha granulosa*) and palatability to predatory dragonflies. *Toxicon*. **57**, 978–983 (2011).

33. A. N. Stokes, B. L. Williams, S. S. French, An improved competitive inhibition enzymatic immunoassay method for tetrodotoxin quantification. *Biol. Proced. Online*. **14**, 3 (2012).

34. C. T. Hanifin, E. D. Brodie III, E. D. Brodie, Jr., Tetrodotoxin levels of the rough-skin newt, *Taricha granulosa*, increase in long-term captivity. *Toxicon*. **40**, 1149–1153 (2002).

35. C. T. Hanifin, E. D. Brodie III, E. D. Brodie, Jr., A predictive model to estimate total skin tetrodotoxin in the newt *Taricha granulosa*. *Toxicon*. **43**, 243–249 (2004).

36. M. T. J. Hague *et al.*, Toxicity and population structure of the Rough-Skinned Newt (*Taricha granulosa*) outside the range of an arms race with resistant predators. *Ecol. Evol.* **6**, 2714–2724 (2016).

37. S. A. Murray, T. K. Mihali, B. A. Neilan, Extraordinary conservation, gene loss, and positive selection in the evolution of an ancient neurotoxin. *Mol. Biol. Evol.* **28**, 1173–1182 (2010).

38. E. D. Brodie III, E. D. Brodie, Jr., Tetrodotoxin resistance in garter snakes: an evolutionary response of predators to dangerous prey. *Evolution*. **44**, 651–659 (1990).

39. B. J. Ridenhour, E. D. Brodie III, E. D. Brodie, Jr., Resistance of neonates and field-collected garter snakes (*Thamnophis* spp.) to tetrodotoxin. *J. Chem. Ecol.* **30**, 143–154 (2004).

40. B. Ridenhour, thesis, Indiana University, Bloomington, IN (2004).

41. M. Lynch, B. Walsh, others, *Genetics and analysis of quantitative traits* (Sinauer Sunderland, MA, 1998), vol. 1.

42. D. Bates, M. Mächler, B. Bolker, S. Walker, Fitting linear mixed-effects models using lme4. *J. Stat. Softw.* **67**, 1–48 (2015).

43. G. Cumming, S. Finch, Inference by eye: Confidence intervals and how to read pictures of data. *Am. Psychol.* **60**, 170–180 (2005).

44. B. Vicoso, J. Emerson, Y. Zektser, S. Mahajan, D. Bachtrog, Comparative sex chromosome genomics in snakes: differentiation, evolutionary strata, and lack of global dosage compensation. *PLoS Biol.* **11**, e1001643 (2013).

45. B. Augstenová *et al.*, ZW, XY, and yet ZW: Sex chromosome evolution in snakes even more complicated. *Evolution*. **72**, 1701–1707 (2018).

46. M. Stephens, N. J. Smith, P. Donnelly, A new statistical method for haplotype reconstruction from population data. *Am. J. Hum. Genet.* **68**, 978–989 (2001).

47. J. Graffelman, J. Morales-Camarena, Graphical tests for Hardy-Weinberg Equilibrium based on the ternary plot. *Hum. Hered.* **65**, 77–84 (2008).

48. J. Graffelman, B. S. Weir, Multi-allelic exact tests for Hardy–Weinberg equilibrium that account for gender. *Mol. Ecol. Resour.* **18**, 461–473 (2018).

49. J. Graffelman, B. S. Weir, On the testing of Hardy-Weinberg proportions and equality of allele frequencies in males and females at biallelic genetic markers. *Genet. Epidemiol.* **42**, 34–48 (2018).

50. J. Graffelman, B. Weir, Testing for Hardy–Weinberg equilibrium at biallelic genetic markers on the X chromosome. *Heredity*. **116**, 558 (2016).

51. L. Excoffier, H. E. L. Lischer, Arlequin suite ver 3.5: a new series of programs to perform population genetics analyses under Linux and Windows. *Mol. Ecol. Resour.* **10**, 564–567 (2010).

52. B. K. Peterson, J. N. Weber, E. H. Kay, H. S. Fisher, H. E. Hoekstra, Double digest RADseq: An inexpensive method for de novo SNP discovery and genotyping in model and non-model species. *PLoS ONE*. **7**, e37135–11 (2012).

53. S. Andrew, *FastQC* (2016; https://www.bioinformatics.babraham.ac.uk/projects/fastqc/).

54. J. Catchen, P. A. Hohenlohe, S. Bassham, A. Amores, W. A. Cresko, Stacks: an analysis tool set for population genomics. *Mol. Ecol.* **22**, 3124–3140 (2013).

55. B. Langmead, S. L. Salzberg, Fast gapped-read alignment with Bowtie 2. *Nat. Methods*. **9**, 357–359 (2012).

56. B. Gruber, P. J. Unmack, O. F. Berry, A. Georges, dartr: An r package to facilitate analysis of SNP data generated from reduced representation genome sequencing. *Mol. Ecol. Resour.* (2017).

57. R Core Team, *R: A Language and Environment for Statistical Computing* (R Foundation for Statistical Computing, Vienna, Austria, 2018; https://www.R-project.org/).

58. M. Foll, O. Gaggiotti, A genome-scan method to identify selected loci appropriate for both dominant and codominant markers: a Bayesian perspective. *Genetics*. **180**, 977–993 (2008).

59. M. Nei, *Molecular evolutionary genetics* (Columbia University Press, 1987).

60. J. Goudet, T. Jombart, *hierfstat: Estimation and Tests of Hierarchical F-Statistics* (2015; https://CRAN.R-project.org/package=hierfstat).

61. B. S. Weir, C. C. Cockerham, Estimating F-statistics for the analysis of population structure. *evolution*. **38**, 1358–1370 (1984).

62. L. W. Pembleton, N. O. I. Cogan, J. W. Forster, StAMPP: an R package for calculation of genetic differentiation and structure of mixed-ploidy level populations. *Mol. Ecol. Resour.* **13**, 946–952 (2013).

63. F. Rousset, Genetic differentiation and estimation of gene flow from F-statistics under isolation by distance. *Genetics*. **145**, 1219–1228 (1997).

64. P. Legendre, M.-J. Fortin, Comparison of the Mantel test and alternative approaches for detecting complex multivariate relationships in the spatial analysis of genetic data. *Mol. Ecol. Resour*. **10**, 831–844 (2010).

65. P. G. Meirmans, Seven common mistakes in population genetics and how to avoid them. *Mol. Ecol.* **24**, 3223–3231 (2015).

66. J. Oksanen *et al.*, *vegan: Community Ecology Package* (2018; https://CRAN.R-project.org/package=vegan).

67. J. K. Pritchard, M. Stephens, P. Donnelly, Inference of population structure using multilocus genotype data. *Genetics*. **155**, 945–959 (2000).

68. D. Falush, M. Stephens, J. K. Pritchard, Inference of population structure using multilocus genotype data: linked loci and correlated allele frequencies. *Genetics*. **164**, 1567–1587 (2003).

69. D. A. Earl, B. M. vonHoldt, STRUCTURE HARVESTER: a website and program for visualizing STRUCTURE output and implementing the Evanno method. *Conserv. Genet. Resour*. **4**, 359–361 (2012).

70. G. Evanno, S. Regnaut, J. Goudet, Detecting the number of clusters of individuals using the software structure: a simulation study. *Mol. Ecol.* **14**, 2611–2620 (2005).

71. M. Jakobsson, N. A. Rosenberg, CLUMPP: a cluster matching and permutation program for dealing with label switching and multimodality in analysis of population structure. *Bioinformatics*. **23**, 1801–1806 (2007).

72. R. M. Francis, pophelper: An R package and web app to analyse and visualise population structure. *Mol. Ecol. Resour.* **17**, 27–32 (2017).

73. B. F. J. Manly, Randomization and regression methods for testing for associations with geographical, environmental and biological distances between populations. *Res. Popul. Ecol.* **28**, 201–218 (1986).

74. P. E. Smouse, J. C. Long, R. R. Sokal, Multiple regression and correlation extensions of the mantel test of matrix correspondence. *Syst. Zool.* **35**, 627 (1986).

75. P. Legendre, F.-J. Lapointe, P. Casgrain, Modeling brain evolution from behavior: a permutational regression approach. *Evolution*. **48**, 1487–1499 (1994).

76. J. W. Lichstein, Multiple regression on distance matrices: a multivariate spatial analysis tool. *Plant Ecol.* **188**, 117–131 (2007).

77. E. B. Rosenblum, Convergent evolution and divergent selection: lizards at the White Sands ecotone. *Am. Nat.* (2005).

78. N. Raufaste, F. Rousset, Are partial mantel tests adequate? *Evolution.* **55**, 1703–1705 (2001).

79. F. Rousset, D. Waller, Partial Mantel tests: reply to Castellano and Balletto. *Evolution.* **56**, 1874–1875 (2002).

80. J. M. Szymura, N. H. Barton, Genetic analysis of a hybrid zone between the fire-bellied toads, *Bombina bombina* and *B. variegata*, near Cracow in southern Poland. *Evolution*. **40**, 1141–1159 (1986).

81. J. M. Szymura, N. H. Barton, The genetic structure of the hybrid zone between the fire-bellied toads *Bombina bombina* and *B. variegata*: comparisons between transects and between loci. *Evolution*. **45**, 237–261 (1991).

82. E. P. Derryberry, G. E. Derryberry, J. M. Maley, R. T. Brumfield, HZAR: hybrid zone analysis using an R software package. *Mol. Ecol. Resour.* **14**, 652–663 (2014).

83. D. T. Baldassarre, T. A. White, J. Karubian, M. S. Webster, Genomic and morphological analysis of a semipermeable avian hybrid zone suggests asymmetrical introgression of a sexual signal. *Evolution.* **68**, 2644–2657 (2014).

84. E. S. Scordato *et al.*, Genomic variation across two barn swallow hybrid zones reveals traits associated with divergence in sympatry and allopatry. *Mol. Ecol.* **26**, 5676–5691 (2017).

85. J. Fox, S. Weisberg, *An R companion to applied regression* (Sage, Thousand Oaks CA, Second., 2011; http://socserv.socsci.mcmaster.ca/jfox/Books/Companion).

86. S. Nakagawa, H. Schielzeth, A general and simple method for obtaining R^2 from generalized linear mixed-effects models. *Methods Ecol. Evol.* **4**, 133–142 (2013).

87. K. Bartoń, *MuMIn: Multi-Model Inference* (2018; https://CRAN.R-project.org/package=MuMIn).

Acknowledgements:

We thank the Departments of Fish and Wildlife in Washington and Oregon for scientific collecting permits to MTJH (18-082 and 063-18, respectively). We also thank IACUC for the protocol to EDB Jr. at USU (1008). We are grateful for Tanner St. Pierre's help with fieldwork. R. Cox, D. Taylor, A. Bergland, D. Carr, and the Brodie and Feldman lab groups provided helpful comments that improved this manuscript. **Funding**: This work was supported by a Doctoral Dissertation Improvement Grant from the National Science Foundation to MTJH and EDB III (DEB 1601296). **Author contributions**: MTJH designed the project, collected specimens, generated genetic data, and performed statistical analyses. ANS collected phenotypic data on newt TTX levels. CRF collected specimens and phenotypic data on snake resistance. EDB Jr. collected phenotypic data on snake resistance and provided leadership on the project. EDB III designed the project and provided leadership. All authors prepared the manuscript. **Competing interests**: The authors declare no conflict of interest with this manuscript. **Data and materials availability**: DNA sequence alignments for the DIV p-loop of $Na_V1.4$ and the ddRADseq data will be made available on GenBank upon manuscript acceptance. All phenotypic data and the code for statistical analyses will be submitted to Dryad upon acceptance.

391 **List of Supplementary Materials:**

392 Materials and Methods

393 Supplementary Text

394 Figures S1-S2

395 Tables S1-S5

396 References (*32-87*)

Fig. 1. Matching phenotypes in prey and predator imply arms race coevolution. (**A**) Population means of TTX levels (μg/cm^2) in newts and (**B**) phenotypic TTX resistance (50% MAMU dose) in snakes along the latitudinal transect. Error bars indicate 95% confidence intervals. The x-axis represents linear distance (km) from the northernmost sampling site (Clallam; 0 km). For snakes, the frequency of TTX-resistant alleles in the $Na_V1.4$ channel is shown with pie charts proportional to sample size. To the right, the schematic of $Na_V1.4$ shows the four domains of the channel (DI–DIV), with the extracellular pore loops (p-loops) highlighted with bold lines. Specific amino acid changes in the DIV p-loop are shown in their relative positions within the pore. The TTX-sensitive ancestral sequence (purple) is listed, followed by the two derived alleles known to confer increases in channel resistance in this lineage. (**C**) Map inset illustrates population estimates of prey toxins and predator resistance at each location in the geographic mosaic. Blue colors correspond to low estimates of TTX (squares) or resistance (circles), whereas red indicates escalated phenotypes in the arms race.

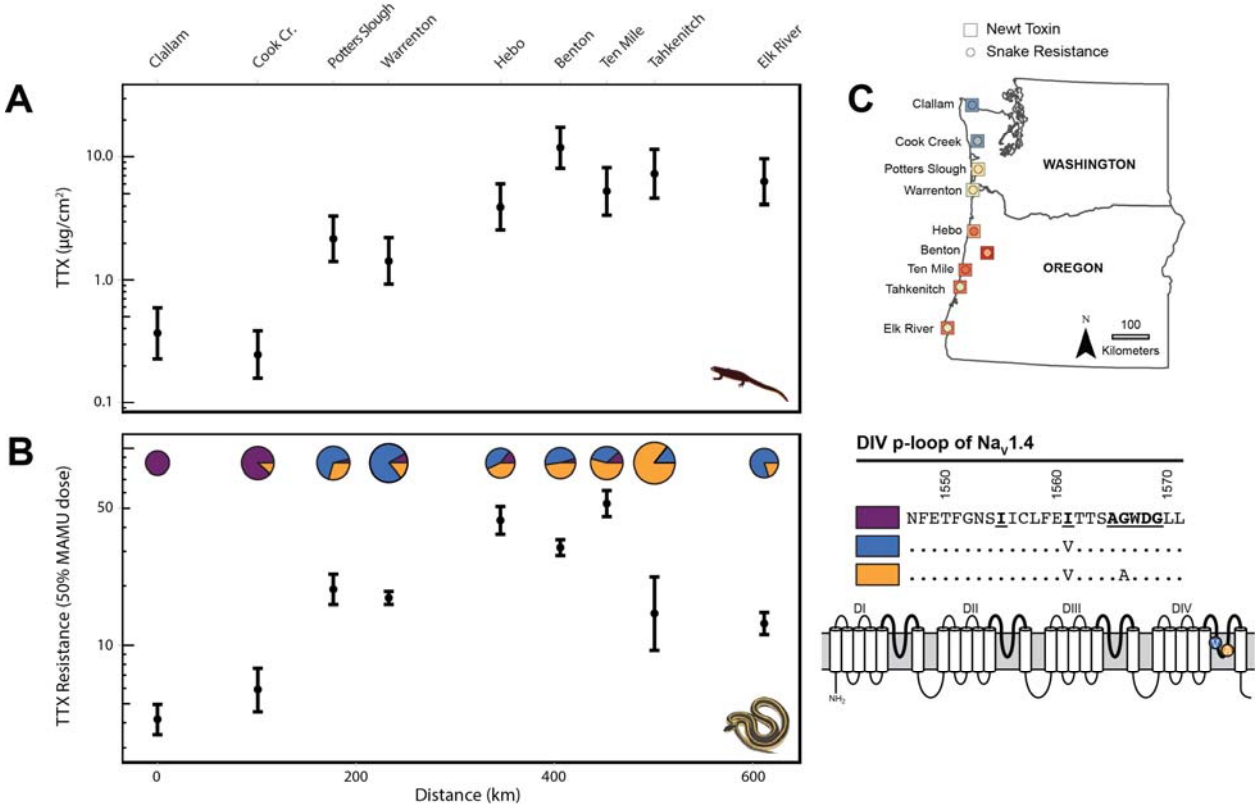

411 **Fig. 2. Populations of prey and predator differ in geographic structure.** Results from the
412 principal coordinate (PCoA) and STRUCTURE analyses of neutral SNPs from newts and
413 snakes. PCoA graphs are rotated 90º to emphasize the major axis of variation corresponding to
414 latitude. The PC 1 values for each individual were used as a neutral expectation in the cline-
415 fitting analyses. STRUCTURE plots are arranged latitudinally by population, in the same order
416 as the map. Each horizontal bar represents the ancestry assignment of an individual, with
417 populations separated by white dashed lines.

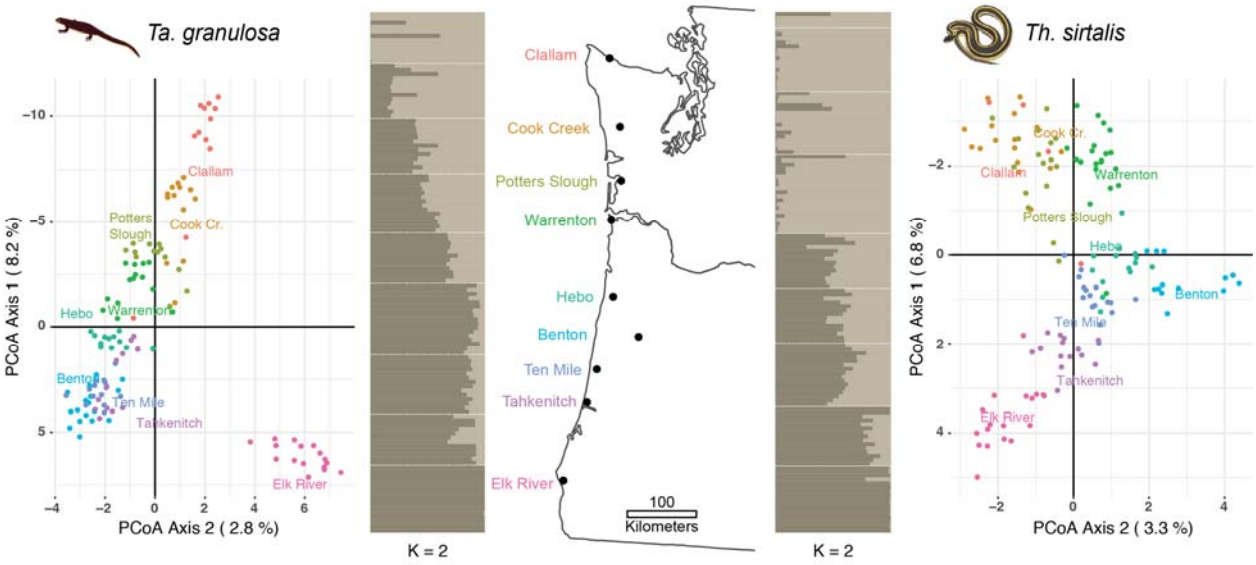

418

Fig. 3. Levels of prey toxin are best predicted by neutral population structure, whereas predator resistance is predicted by prey toxins. Cline-fitting results for phenotypic and genetic variation are shown, with error bars indicating confidence intervals surrounding the geographic cline centers. (**A**) Phenotypic clines of TTX levels (log[TTX μg/cm^2 + 0.1]) and (**B**) TTX resistance (ln[MAMU + 1]) are shown in red. For snakes, the frequency of TTX-resistant alleles in the $Na_V1.4$ channel was also modeled (in black). Gray dashed lines represent the neutral expectation for trait variation due to population structure, based on the PCoA. The cline center points of TTX levels and neutral PC 1 in newts, and phenotypic resistance and TTX-resistant alleles in snakes, are all located within in 84 km of each other along the 611 km transect.

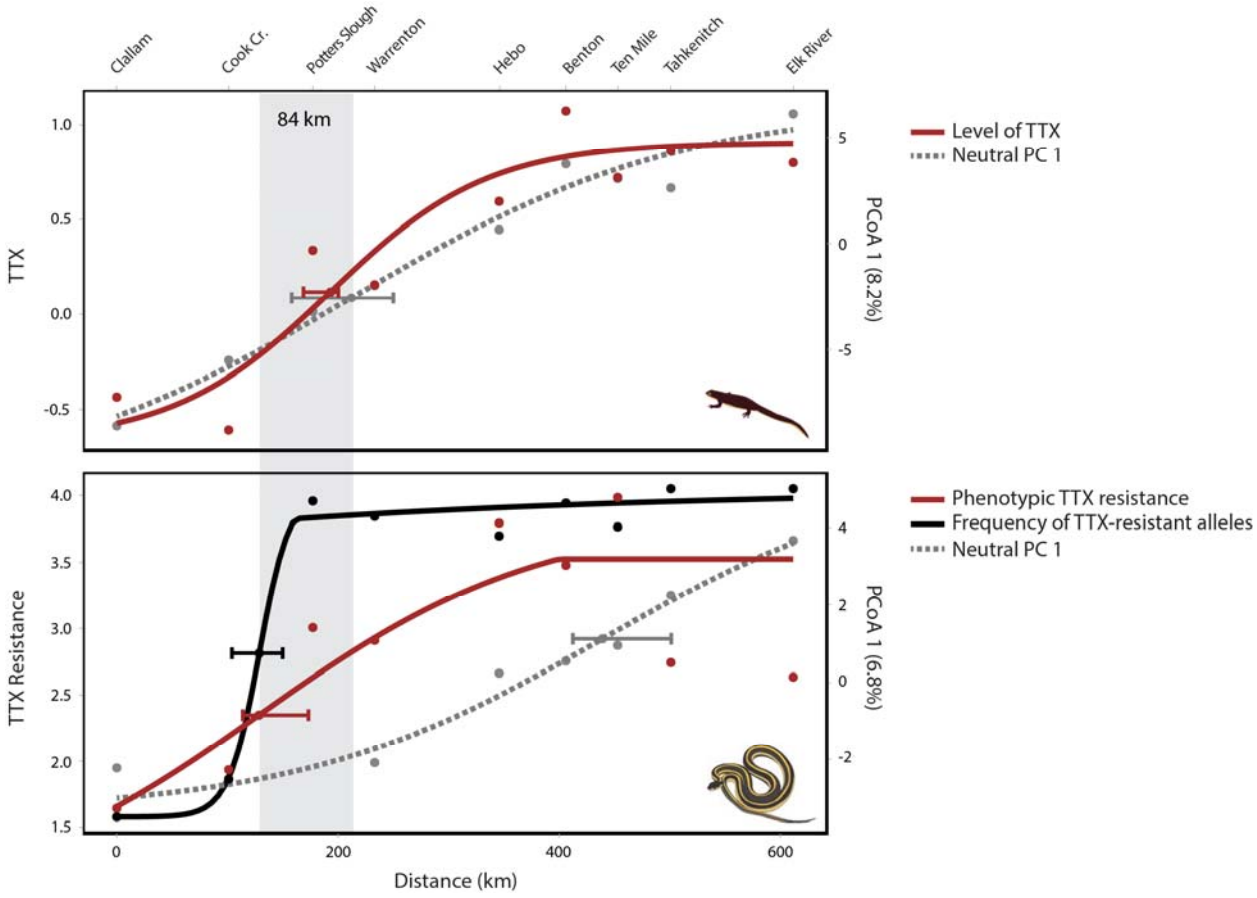

Table 1. Results from multiple regression of distance matrices (MRMs) comparing population divergence in phenotypic and genetic data.

Response Variable	Explanatory Variable(s)	Coefficient	p-value	R^2
Newt TTX levels	Neutral F_{ST} of newts	5.998	**0.002***	0.414
	TTX resistance of snakes	0.415	**0.019***	0.274
	Neutral F_{ST} + TTX resistance			
	Neutral F_{ST} of newts	4.827	**0.006***	0.501
	TTX resistance of snakes	0.253	0.065˙	
Snake TTX resistance	Neutral F_{ST} of snakes	1.442	0.719	0.006
	TTX level of newts	0.662	**0.021***	0.274
	Neutral F_{ST} + TTX toxicity			
	Neutral F_{ST} of snakes	-5.830	0.189	0.338
	TTX level of newts	0.873	**0.011***	
	Neutral F_{ST} of newts	4.632	**0.035***	0.155
Snake F_{ST} of DIV p-loop	Neutral F_{ST} of snakes	2.649	0.202	0.080
	Neutral F_{ST} of newts	3.196	**0.010***	0.311